*Korean J. Chem. Eng.*, 40(11), 2683-2691 (2023)
DOI: 10.1007/s11814-023-1467-2

pISSN: 0256-1115
eISSN: 1975-7220

# Comparative study of enhanced catalytic properties of clay-derived $SiO_2$ catalysts for biodiesel production from waste chicken fat

**Iqra Riaz*, Obaid Ali Qamar*, Farrukh Jamil*,†, Murid Hussain*,†, Abrar Inayat**,***, Lisandra Rocha-Meneses**, Parveen Akhter****, Sara Musaddiq*****, Muhammad Ramzan Abdul Karim******, and YoungKwon Park*******,†**

*Department of Chemical Engineering, COMSATS University Islamabad, Lahore Campus, Defence Road, Off Raiwind Road, Lahore 54000, Pakistan
**Biomass & Bioenergy Research Group, Center for Sustainable Energy and Power Systems Research, Research Institute of Sciences and Engineering, University of Sharjah, 27272 Sharjah, United Arab Emirates
***Department of Sustainable and Renewable Energy Engineering, University of Sharjah, 27272 Sharjah, United Arab Emirates
****Department of Chemistry, The University of Lahore, 1-km Defence Road, Off Raiwind Road, Lahore, Pakistan
*****Department of Chemistry, The Women University Multan, Kutchery Campus, Multan 66000, Pakistan
******Faculty of Materials and Chemical Engineering, Ghulam Ishaq Khan Institute of Engineering Sciences and Technology, Topi, 23640, Pakistan
*******School of Environmental Engineering, University of Seoul, Seoul 02504, Korea
(*Received 20 December 2022 • Revised 16 March 2023 • Accepted 7 April 2023*)

**Abstract**−The use of biodiesel is a proactive measure that can be implemented to reduce emissions of greenhouse gases and other adverse environmental impacts. However, one of the major setbacks to biodiesel production is its relatively higher cost compared to petroleum diesel. The optimistic solution to this is valorization of biomasses like waste chicken fat (WCF) and clay for deriving non-edible oil and catalyst respectively. Herein, we report the synthesis of clay derived $SiO_2$ catalyst impregnated with SrO, $Bi_2O_3$, CuO and CaO. The developed catalysts were characterized by FTIR, XRD, and SEM. XRD studies confirmed the successful impregnation of active metallic oxide on $SiO_2$ support. Further, these catalysts were employed for biodiesel production from WCF, and $SrO/SiO_2$ was found to be most effective and efficient catalyst for biodiesel production from WCF. Hence, $SrO/SiO_2$ was adapted to optimize the different transesterification reaction parameters such as methanol to oil ratio, catalyst loading, reaction temperature and time. The optimized conditions for maximum biodiesel yield 98.9% were found to be 65 °C in 1 h with 12 : 1 methanol to oil ratio and 1 wt% catalyst loading. The biodiesel produced was also analyzed by GC-MS. The obtained biodiesel yield shows that clay can be a potential, and cost-effective, catalyst source to produce biodiesel from WCF.

Keywords: Biodiesel, Transesterification, Heterogeneous Catalyst, Animal Fat

## INTRODUCTION

Energy has been continuously consumed by different sectors to enhance the human lifestyle [1-4]. That is why fossil fuels are rapidly consumed for energy generation to meet energy demand. But fossil fuels (non-renewable) have limitations in terms of environmental safety and economics [5-8]. Hence, the development of an appropriate and long-term alternative to fossil fuels is required owing to their high cost, which has become a serious economic obstacle [9,10]. These long-term sustainable resources are renewable, such as wind, geothermal, solar, waves, and biomass, which are easily available, cost effective, and environment friendly [11-14]. Biomass resources are the most shining stars in reducing toxic emissions by fossil fuels. Biomass can produce renewable energy like biofuels and replace fossil fuels [15-17].

Biodiesel fuel (BDF) is a sustainable form of energy that can contribute to the reduction of carbon dioxide as well as other greenhouse pollutants [18,19]. It has the potential to fulfil the energy needs of the world's most important industries, including those that deal in transportation, agriculture, commerce, and industrial resources [20-22]. Because of its one-of-a-kind properties, such as a higher viscosity than regular diesel, a higher energy content as a result of having no sulfur content, and a higher cetane number, which creates low emissions, it is a superior alternative to regular diesel [23,24]. Edible and non-edible oils are different feedstocks for producing biodiesel [25,26]. Furthermore, non-edible oil has risen to the forefront of this field because of its ability to circumvent the food-versus-fuel conundrum that is caused by edible oils [27]. The type of feedstock that is utilized is the primary contributor to economic considerations, each of which has the potential to have a significant impact on the cost of producing biodiesel [28,29]. Because of this, the production cost can be decreased by the utilization of feedstocks obtained from non-edible oils and biomass (cheaper feed-

†To whom correspondence should be addressed.
E-mail: fjamil@cuilahore.edu.pk, drmhussain@cuilahore.edu.pk, ykpark0426@gmail.com

stock). Eventually, choosing feedstock becomes a significant factor in biodiesel production [30].

Waste chicken fat (WCF) can be found in different sectors like hotels, restaurants, slaughter-houses, and farming businesses [31]. WCF is not directly utilized by humans and is thrown out openly, generating a variety of health and environmental issues [32]. To alleviate these problems, it is preferable to implement strategies that involve the valorization of wastes of this kind in order to produce a variety of useful products [33]. As reported in the literature, WCF is mostly made up of free fatty acids and triglycerides and considered as a most attractive source for producing biodiesel [34]. Biodiesel made from WCF provides a number of advantages over conventional biodiesel, including lower emissions and a higher cetane number [35]. In addition, the biodiesel that is created through the utilization of WCF possesses a quality known as oxidative stability. The process of transesterification, which entails the subsequent extraction of oil from WCF after the oil has been extracted, is uncomplicated and economical [36]. This reaction results in methyl esters with glycerol as by-product upon reaction of triglycerides and methanol at appropriate conditions. Particularly, adopting different catalysts can enhance the rate of transesterification reaction [37,38]. There has been a significant amount of research done on homogeneous and heterogeneous catalysis for the purpose of optimizing the yield of biodiesel. However, heterogeneous catalysts are currently in the spotlight due to their separability, reusability, and relatively low cost [39,40]. However, the synthetic methods of producing heterogeneous catalysts are not only unsuitable but also expensive from an industrial point of view [41-43]. Hence, nanocatalysts obtained from cheaper feedstocks are gaining interest [44-46].

Clay is easily accessible and a promising source of $SiO_2$, an active catalyst for producing biodiesel [47,48]. The lone $SiO_2$ is neither stable nor active because it takes such a long time to achieve equilibrium conversion [49]. There are several publications available in the literature that concentrate on improving the properties of $SiO_2$ through the application of a variety of various chemical and physical techniques [50-53]. It is also possible to draw the conclusion that activity and stability of $SiO_2$ can be increased through different active metal oxides. The loading with suitable metal oxide considerably improves the characteristics of the catalytic processes. The metallic oxide particles strain because of the strong connection between the metal and the support, which strengthens the catalytic behavior. The addition of suitable metallic oxide, on the other hand, can also improve the basic characteristics of the surface. Hence, herein, we report and investigate the catalytic properties of clay derived $SiO_2$ impregnated with four metallic oxides (SrO, $Bi_2O_3$, CaO and CuO). To the best of our knowledge, there has been no report on investigating the catalytic properties of clay derived $SiO_2$ impregnated with these metallic oxides in a comparative manner. The prepared catalysts were further used for trans-esterification of WCF oil. Also, this paper emphasizes the optimization of various parameters for producing biodiesel from oil obtained from WCF.

## MATERIALS AND METHODS

### 1. Materials

The clay samples were collected at COMSATS University Islamabad Lahore campus (gardening area) to prepare the catalyst base. Strontium, calcium, copper, and bismuth salts were purchased from Merck, UK. For the delamination of the Clay or $SiO_2$ extraction, $H_2SO_4$, HCl, $HNO_3$, and $CH_3COOH$ were used. WCF for biodiesel production was obtained from a local shop.

### 2. Synthesis of Catalysts

The precursor $SiO_2$ was prepared by washing 100 g of clay with distilled water and stirring at 500 rpm for 8 h. Washed clay was filtered and further dried for 4 h at 110 °C. To delaminate the clay samples (20 g each), they were stirred with four different acid solutions (0.2 N) of HCl, $H_2SO_4$, $HNO_3$, and $CH_3COOH$, for 4 h. The samples were filtered followed by washing with DI-water to neutralize the pH and dried at 110 °C for 4 h. Finally, four samples of precursor $SiO_2$ were prepared by treatment with four different acids. The active metal impregnation method used for the final catalyst was as follows. The solutions (4 wt%) of desired salts (strontium chloride, calcium chloride, copper chloride, and bismuth nitrate) were prepared by dissolving them in appropriate quantity of distilled water and slowly dispersed on $SiO_2$ support drop by drop. The obtained slurry was dried in oven at 80 °C to let the water evaporate followed by calcination at required temperatures for all precursors. The prepared catalysts were characterized by XRD, FT-IR, SEM and used for transesterification of WCF.

### 3. Catalyst Characterization

XRD was performed using a Rigaku diffractometer in $2\theta$ angle range of 5-80° with a 2° step size. An FT-IR spectrophotometer (Perkin Elmer Frontier) was used to identify the surface groups of the catalysts in the wavenumber range of IR spectra (700-4,000 $cm^{-1}$). The morphology was studied using SEM.

### 4. Biodiesel Production

The collected WCF underwent washing and cleaning before extraction of oil. The washing and cleaning were achieved by using distilled water to remove dust particles and other odorous wastes five times. The washed and cleaned WCF (300 g) was melted at 65 °C to convert it into liquid oil. The suspension was then filtered, centrifuged, and decanted to remove the suspended particles. The transesterification process was carried out in a 500 mL three-neck round bottom flask connected to a reflux condenser and thermocouple. After proper mixing of catalyst in methanol, the oil was heated at 60 °C, utilizing a round-bottom flask with stirring. After the completion of the reaction, the product was filtered and poured into a separating funnel. After 24 h settling time, biodiesel and glycerol layers formed, and the biodiesel was separated. Reaction parameters were investigated in different ranges 6 : 1 to 14 : 1 (methanol to oil ratio), 1 to 5 wt% (catalysts loadings), 55 to 70 °C (temperature) and 0.5 to 3 h (time). The steps involved in biodiesel production can been seen in Fig. 1.

The composition of FAME in the reaction products was found by GC-MS (GC: Agilent 6890N and MS: 5973N) with an inert mass selective detector (model 5975). The DB1 (30 m×0.32 mm×0.1 μm) as capillary column, and helium carrier-gas was used. The flow rate of helium gas was 10 mL $min^{-1}$. The yield was calculated using Eq. (1).

$$\text{Biodiesel Yield (\%)} = \frac{\text{Weight of produced FAME}}{\text{Weight of used oil}} \times 100 \quad (1)$$

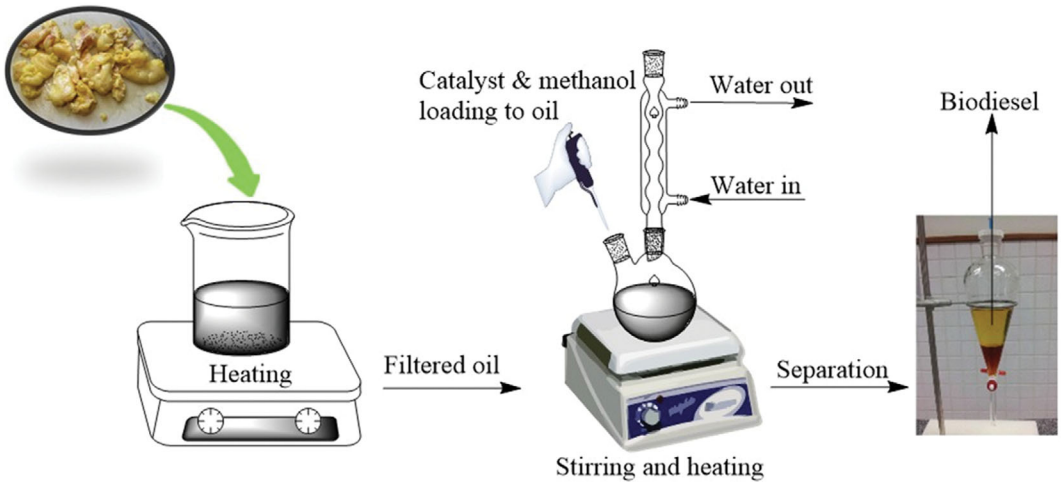


**Fig. 1. The different steps adopted in biodiesel production.**

## RESULTS AND DISCUSSION

### 1. Catalyst Characterization

1-1. XRD Studies

The XRD pattern of the precursor silica and four catalysts are shown in Fig. 2. The bottom spectra represent the profiles of the untreated/original clay. The peak of clay treated with acids show a high-intensity peak of silica $SiO_2$. The strong acid resulted in a high reflection at $2\theta$ values of $SiO_2$ particles at 26.52°. For the modified samples of the synthesized catalyst, the peaks representing the metal oxides are encircled. It can be observed that acid treatment did not change the phase of the catalyst; moreover, no additional peak was present in the spectra representing the clay samples modified with acids. It can be seen in SrO-$SiO_2$ spectra, there was an additional peak at 30.4°. SrO catalyst shows prominent reflection peaks at $2\theta$=30.31, 50.54°, and 63.04 [54-56]. Further on, the spectrum representing $SiO_2$ modified with bismuth oxide shows an additional peak at 27.1°. Similarly, the spectra representing addition of CaO and CuO show additional peaks for pristine silica dioxide at 20.9° and 41.2°, respectively. The diffraction pattern of CaO reveals enhanced peaks at $2\theta$=37.3° and 53.8° [57]. The bismuth silicate crystal catalyst structure was examined, and initial diffraction peaks centered at range of 20-68° and reported at 21°, 27.5°, 32.6°, 34.9°, 43.0°, 44.9°, 51.8°, 55.0°, 56.6°, 58.1°, 61.1°, 62.6°, 64.0°, 66.8°, and 68.2° crystal planes of crystalline cubic phase of $Bi_4Si_3O_{12}$ [58]. It can be seen clearly that pure $SiO_2$ contains no additional peaks of metallic oxides. Meanwhile, the impregnated catalysts show additional peaks of corresponding metallic oxides, which shows the successful impregnation of metallic oxides on $SiO_2$ support.

1-2. FTIR Studies

FTIR spectroscopy allowed for the identification of several functional groups, as shown in Fig. 3. In this O-H stretching region, the band prominent at 3,000-3,750 $cm^{-1}$ and C=O stretching was observed at 1,428 $cm^{-1}$ and 1,702 $cm^{-1}$, O-Si bending at 1,035 $cm^{-1}$,

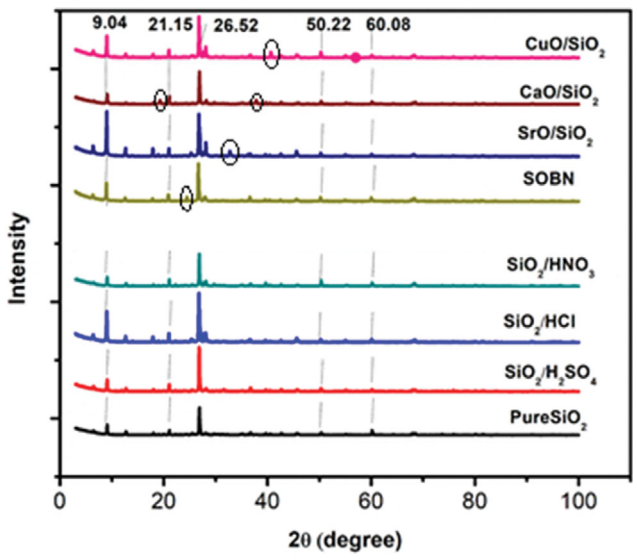


**Fig. 2. XRD characterization of silica-supported catalysts.**

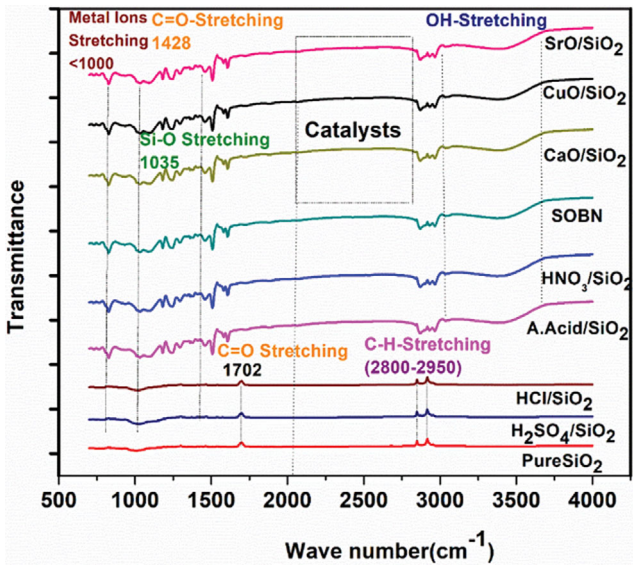


**Fig. 3. FTIR characterization of silica and silica-supported catalysts.**

and C-H stretching at 2,800-2,950 $cm^{-1}$. Peaks at 3,699 $cm^{-1}$, 1,462 $cm^{-1}$, and 1,118 $cm^{-1}$ belong to vibrating carbonate-bond in catalyst, whereas the peaks 3,450 and 1,772 $cm^{-1}$ belong to H-O-H deformation of $H_2O$ physically adsorbed on the surface [59]. The FTIR spectra of $SrO/SiO_2$ and SrO stretching peak at 300-750 $cm^{-1}$ are shown in Fig. 3. Si-O stretching was observed at 1,035 $cm^{-1}$. For $CaO/SiO_2$, Ca-O is responsible for absorption in region 700-900 $cm^{-1}$ [60]. Si-O stretching at approximately 1,035 $cm^{-1}$ was clearly observed for $SiO_2$. O-H stretching was observed at 3,200-3,500 $cm^{-1}$, and the C=O stretching was observed at 1,428 $cm^{-1}$. The bending absorption of the Cu-OH bond was at 690 $cm^{-1}$, indicating the presence of $Cu(OH)_2$ [61]. For $CuO/SiO_2$, CuO bending absorption appeared at 601, 1,350, 1,500, 2,750-2,925 $cm^{-1}$, and Si-O stretching was observed at a wave number of 1,035 $cm^{-1}$. The vibration of the Bi-O bond in a stoichiometric molecule is associated with the 630 $cm^{-1}$ peak. The peaks 415 $cm^{-1}$ and 1,011


**Fig. 4. SEM analysis of (a) $SiO_2$ precursor, (b) $SrO/SiO_2$, (c) $CuO/SiO_2$, (d) $CaO/SiO_2$, and (e) $Bi_2O_3$.**

$cm^{-1}$ belong to vibrating Bi-O bond in oxide $Bi_2O_3$ and Si-O bond, respectively [62]. In this study, $SiO_2$ supported Bismuth oxide catalyst peaks were observed, as shown in Fig. 3. Bi-O bending absorption was observed at 650, 1,000, and 1,250 $cm^{-1}$ with Si-O stretching at 1,035 $cm^{-1}$.

1-3. SEM Analysis

Scanning electron microscopy (SEM) was used to examine the morphology of the synthesized catalysts. The images are shown at high-resolution magnification of up to ×200k. The precursor silica $SiO_2$ shows the crystalline morphology of silica needles, as shown in Fig. 4(a). In the $SrO/SiO_2$ catalyst, SrO particles are distributed on the pristine $SiO_2$ base and display a crystalline morphology (Fig. 4(b)). The $CuO/SiO_2$ catalyst exhibits irregular edges in the long and block crystal morphologies, as shown in Fig. 4(c). $CaO/SiO_2$ catalyst morphology analysis resulted in a spherical porous crystal structure, as shown in Fig. 4(d). Similarly, the $Bi_2O_3/SiO_2$ analysis shows that the aggregated crystalline morphology also formed large holes, as shown in Fig. 4(e).

**2. Product Analysis**

2-1. GC-MS Analysis

Biodiesel was analyzed by using the GC-MS technique to identify unknown ester constituents. GC-MS detected all triglyceride components during transesterification, including myristic acid, palmitic acid, and linoleic acid. The FAMEs were identified using library (GC-MS) investigation to verify the retention time and mass fragmentation. The biodiesel prepared from the $SrO/SiO_2$ catalyst (B1) possessed major esters such as lauric acid, stearic acid, saturated fatty acids, and unsaturated fatty acids, with a retention time range of 11.4-32.7 min. The esters have a specific retention time, which helped us identify the components shown in Fig. 5. The biodiesel prepared from the $Bi_2O_3/SiO_2$ catalyst (B2) had major esters, such as palmitic acid, eicosanoic acid, palmitoleate acid, stearic acid, and unsaturated fatty acids with a retention time range of 11.4-36.6 min. The esters have a specific retention time, which helped us identify the components shown in Fig. 6. The biodiesel prepared from the $CuO/SiO_2$ catalyst (B3) had major esters such as oleic acid, palmitic acid, eicosanoic acid, and unsaturated fatty acids with a retention time range of 10-28.8 min. The esters have a specific retention time, which helped us identify the components shown in Fig. 7. The biodiesel prepared from the $CaO/SiO_2$ catalyst (B4) had major esters such as oleic acid, palmitic acid, eicosanoic acid, and unsaturated fatty acids with a retention time range of 10-28.8 min. The esters have a specific retention time, which helped us identify the components shown in Fig. 8. The GC-MS results of biodiesel produced using four different catalyst B1, B2, B3 and B4 are presented

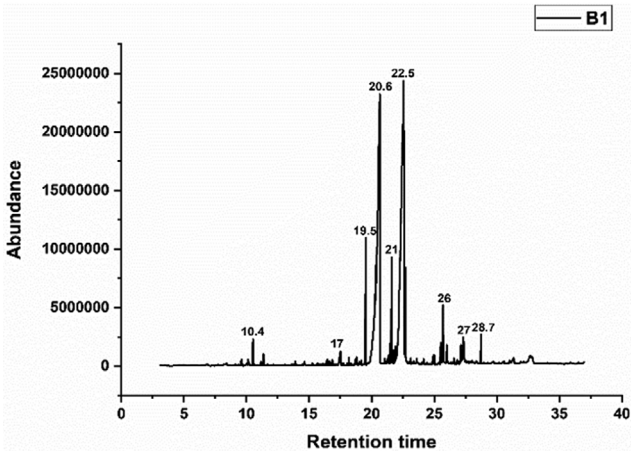


**Fig. 5. GC-MS analysis of B1.**

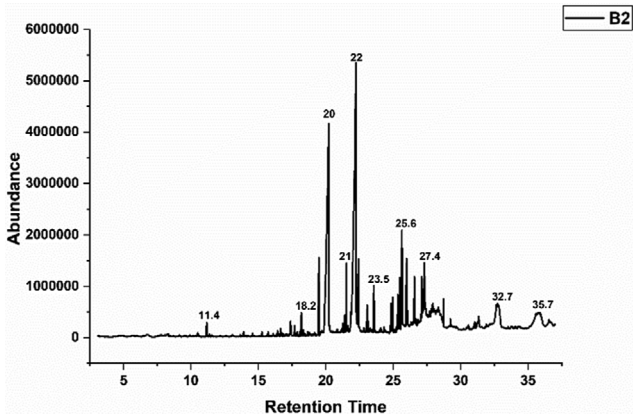


**Fig. 6. GC-MS analysis of B2.**

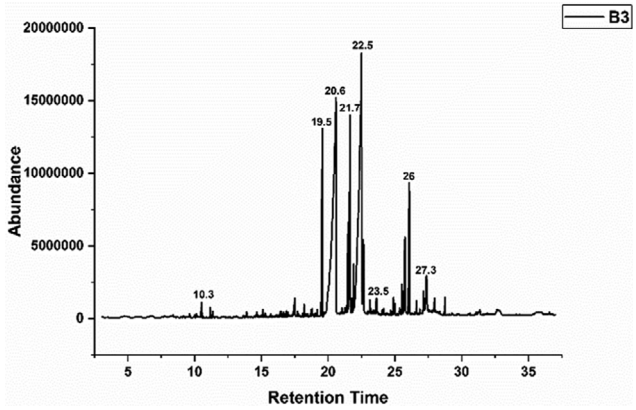


**Fig. 7. GC-MS analysis of B3.**

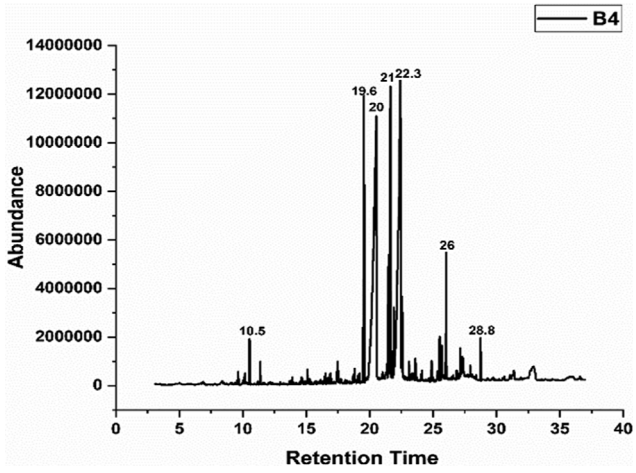


**Fig. 8. GC-MS analysis of B4.**

**Table 1. Composition biodiesel synthesized by four catalysts B1, B2, B3 and B4**

| B1 | | B2 | | B3 | | B4 | |
|---|---|---|---|---|---|---|---|
| Retention time | Composition | Retention time | Composition | Retention time | Composition | Retention time | Composition |
| 10.4 | Lauric | 11.4 | Decadienal | 10.3 | Lauric | 10.5 | Lauric |
| 17 | 2,8-Heptadecanoic | 18.2 | Palmitic | 19.5 | Palmitic | 19.6 | Palmitic |
| 19.5 | Heptadecanoic | 20 | Palmitoleate | 20.6 | Oleic | 20 | Oleic |
| 20.6 | Tetradecanoic | 21 | Heptadecanoic | 21.7 | Heptadecanoic | 21 | Heptadecanoic |
| 21 | Stearic | 22 | Tetradecanoic | 22.5 | Heptacosane | 22.3 | Heptacosane |
| 22.5 | n-Octacosane | 23.5 | Stearic | 23.5 | Docosane | 26 | Tetratetracontane |
| 26 | Saturated Fatty | 25.6 | Tetratetracontane | 26 | Tetratetracontane | 28.8 | Eicosanoic |
| 27 | Octadecadienoic | 27.4 | Eicosanoic | 27.3 | Eicosanoic | | |

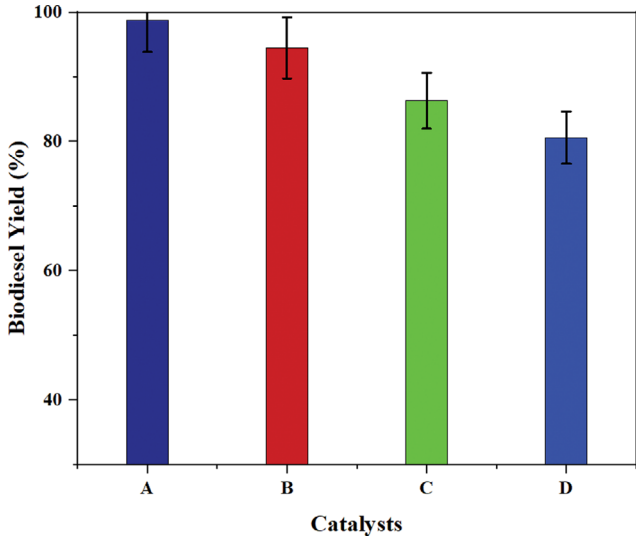


**Fig. 9. Biodiesel yield using different catalysts A ($SrO/SiO_2$), B ($CaO/SiO_2$), C ($CuO/SiO_2$) and D ($Bi_2O_3/SiO_2$).**

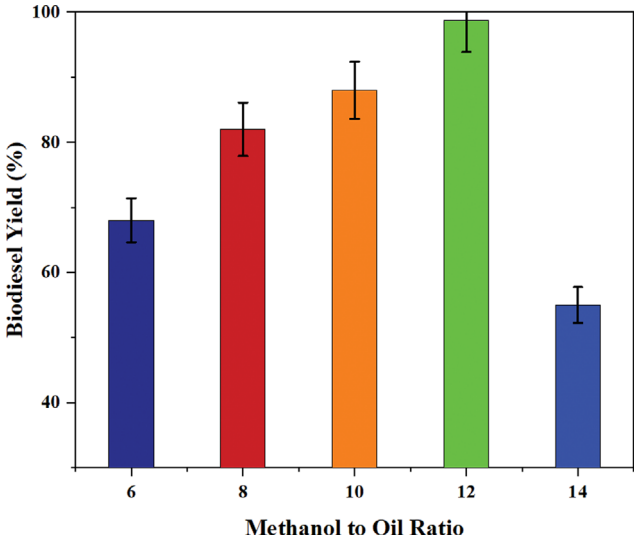


**Fig. 10. Effect of methanol to oil ratio on yield.**

in Table 1.

## 3. Parametric Study

Fig. 9 shows the biodiesel yield obtained from the transesterification of WCF using the four different catalysts, $SrO/SiO_2$, $CaO/SiO_2$, $CuO/SiO_2$ and $Bi_2O_3/SiO_2$. The biodiesel yield was found to be lower (80.6%) for $Bi_2O_3/SiO_2$ among all types of catalysts used in this study. Meanwhile, $CuO/SiO_2$ and $CaO/SiO_2$ produced 86.3% and 94.5% biodiesel. $SrO/SiO_2$ was found to be the more effective and efficient catalyst for maximum biodiesel yield (98.8%) due to enhanced catalytic properties in comparison to all reported catalysts herein. That is why $SrO/SiO_2$ was selected and used for further investigating the effect of different reaction parameters on biodiesel yield.

### 3-1. Methanol-to-oil Ratio

Methanol (alcohol)-to-vegetable oil molar ratio is one of the most important factors affecting ester synthesis. The ratio in the range of 6 : 1-14 : 1 at 65 °C was investigated by keeping the other parameters constant shown in Fig. 10. The reaction was incomplete when the molar ratio was <12 : 1. The biodiesel yield increased with an increase in the methanol-to-oil ratio. Moreover, it decreased when the ratio increased beyond 12. This decline in biodiesel yield at a higher ratio can be due to the phase separation issue of product and by-product, thus tending to decrease the biodiesel yield. Thus, the maximum yield 98.9 wt% was obtained at methanol-to oil-molar ratio of 12.

### 3-2. Catalyst Loadings

The biodiesel yield may have been affected by an inaccurate amount of catalyst. More catalysts lead to inadequate mixing, which causes some catalysts to become unreactive, resulting in a lower conversion. Furthermore, when the amount of catalyst in the mixture was increased, the mixture became thicker, causing mixing issues. Lower yields at low catalyst concentrations can be attributed to incomplete reactions and the consequent difficulty in phase separation due to emulsification [63]. The effect of catalytic activity is shown in Fig. 11, and its performance was analyzed by varying the loading quantity with respect to the oil used. The reaction rate increased to 2 wt% of oil; then it decreased to further loading up to 5 wt% by keeping the other factors constant. The maximum biodiesel yield (98.9 wt%) was obtained when catalyst loading was 1 wt%.

### 3-3. Reaction Time

The reaction time is a significant factor in biodiesel production,

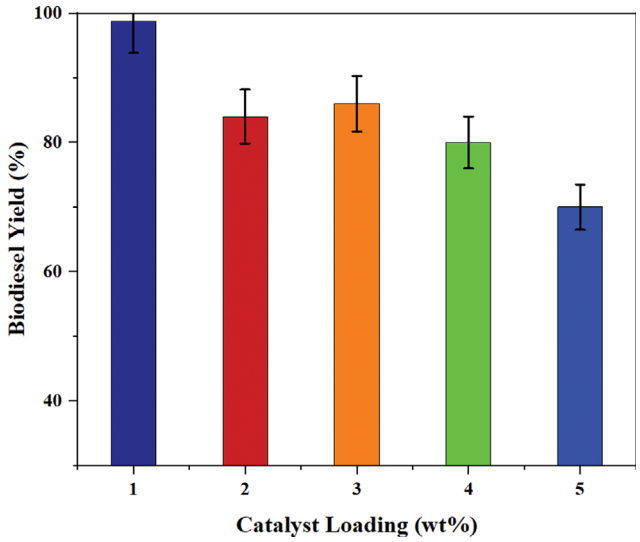


**Fig. 11. Effect of catalyst loadings yield.**

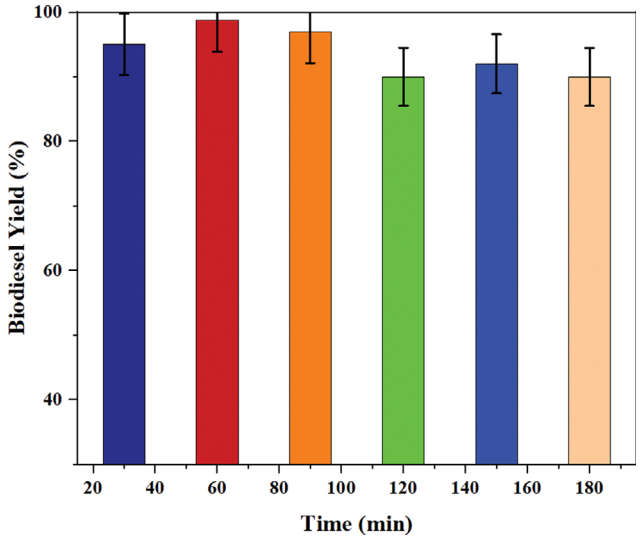


**Fig. 12. Effect of reaction time on yield.**

affecting its yield. As transesterification is an equilibrium reaction, it needs adequate time for reaching equilibrium. Further, there is also need of good contact time for reactants to reach the active sites of catalyst for further reaction. Fig. 12 depicts the effect of reaction time on biodiesel yield. It can be seen that as time was increased to 60 min, a rise in biodiesel yield was found; however, further increase in time showed a decline in biodiesel yield. This can be due to the possibility of reaction occurring in reversible direction. The maximum biodiesel yield (98.9 wt%) was obtained when reaction time was 60 min.

3-4. Reaction Temperature

The biodiesel yield depends upon mass transfer characteristics in the system upon varying temperature [64]. Fig. 13 shows the effect of reaction temperature on biodiesel yield. It can be seen that the yield was lower at 55 °C due to less conversion. However, maximum yield of 98.9% was observed at 65 °C. Upon further increase in temperature, the yield started to drop again due to evaporation of ethanol, resulting in loss of mass transfer in the system.

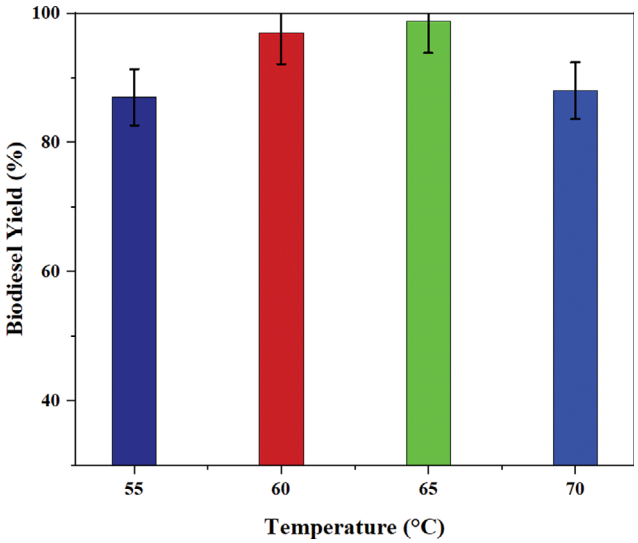


**Fig. 13. Effect of temperature on yield.**

Thus, it can be concluded that the among all synthesized catalysts, SrO-$SiO_2$ can be effectively used as active catalyst for biodiesel production. Based on parametric studies, it can be concluded that the optimum yield of biodiesel was 98.9 wt%. In the presence of a heterogeneous catalyst, the reaction normally follows three steps: The reactants are absorbed on the catalyst, a reaction occurs between the reactants on the active sites, and the last products are desorbed. Therefore, a similar reaction occurred in the current study.

## CONCLUSION

WCF and clay are potential low-cost sources of raw materials for biodiesel production. In this study, four different clay-derived catalysts ($SrO/SiO_2$, $CaO/SiO_2$, $CuO/SiO_2$ and $Bi_2O_3/SiO_2$) were successfully synthesized as biodiesel catalysts. The clay-derived heterogeneous catalysts were suitably employed in the transesterification (valorization) of waste chicken fat that was extracted through a simple non-solvent method. The primary focus of optimization study was on $SrO/SiO_2$ catalyst, which produced the maximum yield among all the synthesized catalysts due to improved catalytic properties. This catalyst shows excellent performance for the conversion of WCF into fatty acids methyl ester/biodiesel. The optimized results show that the maximum yield achieved under reacting conditions was 98.9%. Hence, this work has demonstrated the transesterification of oil from chicken slaughter waste while adopting a cheap, non-solvent process for extraction and subsequently using cheap source of catalyst. Moreover, pilot scale investigation of the process is recommended as future work for adequate and realizable commercialization of the process.

## ACKNOWLEDGEMENT

This work was supported by the Korea Institute of Energy Technology Evaluation and Planning (KETEP) grant funded by

the Korea government (MOTIE) (20210310100020, Production of advanced biofuel from lignocellulosic biomass by a combination of fast pyrolysis and supercritical ethanol upgrading).

## LIST OF ABBREVIATIONS

| | |
|---|---|
| BDF | : biodiesel fuel |
| WCF | : waste chicken fat |
| $H_2SO_4$ | : sulfuric acid |
| $HNO_3$ | : nitric acid |
| $CH_3COOH$ | : acetic acid |
| XRD | : x-ray diffraction |
| FT-IR | : fourier transform infrared |
| SEM | : scanning electron microscopy |
| GC-MS | : gas chromatography mass spectroscopy |

## REFERENCES


1. A. Farooq, S. Moogi, S.-H. Jang, H. P. R. Kannapu, S. Valizadeh, A. Ahmed, S. S. Lam and Y.-K. Park, *J. Ind. Eng. Chem.*, **94**, 336 (2021).
2. H. Zhang, L.-L. Zhang, X. Tan, H. Li and S. Yang, *Ind. Crop. Prod.*, **173**, 114126 (2021).
3. M. Shabir, N. Shezad, I. Shafiq, I. M. Maafa, P. Akhter, K. Azam, A. Ahmed, S. H. Lee, Y.-K. Park and M. Hussain, *J. Ind. Eng. Chem.*, **105**, 539 (2022).
4. S. Pyo, Y.-M. Kim, Y. Park, S. B. Lee, K.-S. Yoo, M. A. Khan, B.-H. Jeon, Y. J. Choi, G. H. Rhee and Y.-K. Park, *J. Ind. Eng. Chem.*, **103**, 136 (2021).
5. H. M. U. Ayub, A. Ahmed, S. S. Lam, J. Lee, P. L. Show and Y.-K. Park, *Bioresour. Technol.*, **344**, 126399 (2022).
6. M. G. Sibi, D. Verma and J. Kim, *Catal. Rev.*, https://doi.org/10.1080/01614940.2022.2099058 (2022).
7. S. U. Hassan, S. Ahmad, M. A. Farid, S. Nadeem, Z. Ali, R. Abro, A. Mohyuddin, M. S. Nazir, M. Hussain and Y.-K. Park, *J. Ind. Eng. Chem.*, **116**, 438 (2022).
8. I. Shafiq, M. Hussain, S. Shafique, R. Rashid, P. Akhter, A. Ahmed, J.-K. Jeon and Y.-K. Park, *J. Ind. Eng. Chem.*, **98**, 283 (2021).
9. C. Sronsri, W. Sittipol and K. U-yen, *Fuel*, **304**, 121419 (2021).
10. F. Jamil, M. Saleem, O. Ali Qamar, M. S. Khurram, A. a. H. Al-Muhtaseb, A. Inayat, P. Akhter, M. Hussain, S. Rafiq, H. Yim and Y.-K. Park, *J. Phys: Energy* (2022).
11. F. Jamil, P. S. Murphin Kumar, L. Al-Haj, M. Tay Zar Myint and A. a. H. Al-Muhtaseb, *Energy Convers. Manage.*, **10**, 100047 (2021).
12. M. Haris Hamayun, M. Hussain, I. Shafiq, A. Ahmed and Y.-K. Park, *Environ. Eng. Res.*, **27**, 200683 (2022).
13. M. Islam Miskat, A. Ahmed, M. S. Rahman, H. Chowdhury, T. Chowdhury, P. Chowdhury, S. M. Sait and Y.-K. Park, *Environ. Eng. Res.*, **26**, 200514 (2021).
14. C. L. Mgbechidinma, G. Zheng, E. B. Baguya, H. Zhou, S. U. Okon and C. Zhang, *Environ. Eng. Res.*, **28**, 220034-0 (2023).
15. U. Shakeel, M. Hussain, R. Sheikh, A. Ahmed, M. S. Nazir, W. Yang, N. Shezad, P. Akhter and Y.-K. Park, *Korean J. Chem. Eng.*, **38**, 966 (2021).
16. A. Abdullah, A. Ahmed, P. Akhter, A. Razzaq, M. Zafar, M. Hussain, N. Shahzad, K. Majeed, S. Khurrum, M. S. A. Bakar and Y.-K. Park, *Korean J. Chem. Eng.*, **37**, 1899 (2020).
17. I. Shafiq, M. Hussain, S. Shafique, M. H. Hamayun, M. Mudassir, Z. Nawaz, A. Ahmed and Y.-K. Park, *Korean J. Chem. Eng.*, **38**, 1768 (2021).
18. I. Riaz, I. Shafiq, F. Jamil, A. H. Al-Muhtaseb, P. Akhter, S. Shafique, Y.-K. Park and M. Hussain, *Catal. Rev.*, https://doi.org/10.1080/01614940.2022.2108197 (2022).
19. K. S. Al-Mawali, A. I. Osman, A. a. H. Al-Muhtaseb, N. Mehta, F. Jamil, F. Mjalli, G. R. Vakili-Nezhaad and D. W. Rooney, *Renew. Energy*, **170**, 832 (2021).
20. A. I. Osman, N. Mehta, A. M. Elgarahy, A. Al-Hinai, A. a. H. Al-Muhtaseb and D. W. Rooney, *Environ. Chem. Lett.*, **19**, 4075 (2021).
21. Q. Zhang, X. Duan, S. Tang, C. Wang, W. Wang, W. Feng and T. Wang, *Environ. Eng. Res.*, **28**, 210560-0 (2023).
22. S. Patnaik, S. Saravanabhupathy, S. Singh, A. Daverey and K. Dutta, *Environ. Eng. Res.*, **27**, 210061-0 (2022).
23. S. F. Basumatary, K. Patir, B. Das, P. Saikia, S. Brahma, B. Basumatary, B. Nath, B. Basumatary and S. Basumatary, *J. Clean. Prod.*, **358**, 131955 (2022).
24. S. Zulkepli, H. V. Lee, N. A. Rahman, L. T. Chuan, P. L. Show, W.-H. Chen and J. C. Juan, *Fuel*, **308**, 121860 (2022).
25. M. Abdul Hakim Shaah, M. S. Hossain, F. A. Salem Allafi, A. Alsaedi, N. Ismail, M. O. Ab Kadir and M. I. Ahmad, *RSC Adv.*, **11**, 25018 (2021).
26. A. a. H. Al-Muhtaseb, A. I. Osman, P. S. Murphin Kumar, F. Jamil, L. Al-Haj, A. Al Nabhani, H. H. Kyaw, M. T. Z. Myint, N. Mehta and D. W. Rooney, *Energy Convers. Manag.*, **236**, 114040 (2021).
27. D. Singh, D. Sharma, S. L. Soni, C. S. Inda, S. Sharma, P. K. Sharma and A. Jhalani, *J. Clean. Prod.*, **307**, 127299 (2021).
28. C. Ningaraju, K. V. Yatish, R. Mithun Prakash, M. Sakar and R. Geetha Balakrishna, *J. Clean. Prod.*, **363**, 132448 (2022).
29. J. W. Roy Chong, X. Tan, K. S. Khoo, H. S. Ng, W. Jonglertjunya, G. Y. Yew and P. L. Show, *Environ. Res.*, **206**, 112620 (2022).
30. N. Chanthon, K. Ngaosuwan, W. Kiatkittipong, D. Wongsawaeng, W. Appamana, A. T. Quitain and S. Assabumrungrat, *Renew. Sust. Energ. Rev.*, **151**, 111430 (2021).
31. M. Ndiaye, A. Arhaliass, J. Legrand, G. Roelens and A. Kerihuel, *Renew. Energy*, **145**, 1073 (2020).
32. N. Liu and J. Jiang, *Biomass Bioenergy*, **143**, 105826 (2020).
33. T. E. Odetoye, J. O. Agu and E. O. Ajala, *J. Environ. Chem. Eng.*, **9**, 105654 (2021).
34. L. Yi-Chia, M. Sekar, A. Chinnathambi, O. Nasif, B. Gavurová, G. K. Jhanani, K. Brindhadevi and N. T. Lan Chi, *Environ. Res.*, **216**, 114742 (2023).
35. M. Saleem, F. Jamil, O. A. Qamar, P. Akhter, M. Hussain, M. S. Khurram, A. a. H. Al-Muhtaseb, A. Inayat and N. S. Shah, *Catalysts*, **12** (2022).
36. N. A. Zul, S. Ganesan, T. S. Hamidon, W.-D. Oh and M. H. Hussin, *J. Environ. Chem. Eng.*, **9**, 105741 (2021).
37. X. Tan, H. Zhang, H. Li and S. Yang, *Fuel*, **310**, 122273 (2022).
38. B. Changmai, C. Vanlalveni, A. P. Ingle, R. Bhagat and S. L. Rokhum, *RSC Adv.*, **10**, 41625 (2020).
39. V. Das, A. M. Tripathi, M. J. Borah, N. T. Dunford and D. Deka, *Renew. Energy*, **161**, 1110 (2020).
40. F. Kesserwan, M. N. Ahmad, M. Khalil and H. El-Rassy, *Chem. Eng. J.*, **385**, 123834 (2020).
41. P. Maheshwari, M. B. Haider, M. Yusuf, J. J. Klemeš, A. Bokhari,

M. Beg, A. Al-Othman, R. Kumar and A. K. Jaiswal, *J. Clean. Prod.*, **355**, 131588 (2022).
42. A. Munyentwali, H. Li and Q. Yang, *Appl. Catal. A: Gen.*, **633**, 118525 (2022).
43. A. Waris, S. Sharif, S. Naz, F. Manzoor, F. Jamil, M. Hussain, Y. J. Choi and Y.-K. Park, *Environ. Eng. Res.*, **28**, 220625 (2023).
44. A. Mukhtar, S. Saqib, H. Lin, M. U. Hassan Shah, S. Ullah, M. Younas, M. Rezakazemi, M. Ibrahim, A. Mahmood, S. Asif and A. Bokhari, *Renew. Sust. Energ. Rev.*, **157**, 112012 (2022).
45. H. Rizqullah, J. Yang and J. W. Lee, *Korean J. Chem. Eng.*, **39**, 2754 (2022).
46. M. Kashif, S. Thangarasu, T. H. Oh, P. Biswas and D. Kang, *Korean J. Chem. Eng.*, **39**, 2652 (2022).
47. U. Zulfiqar, T. Subhani and S. W. Husain, *J. Asian Ceram. Soc.*, **4**, 91 (2016).
48. E. O. Ajala, M. A. Ajala, A. O. Ajao, H. B. Saka and A. C. Oladipo, *Chem. Eng. J. Adv.*, **4**, 100033 (2020).
49. J. Mazarío, J. A. Cecilia, E. Rodríguez-Castellón and M. E. Domine, *Appl. Catal. A: Gen.*, **652**, 119029 (2023).
50. F. Esmi, A. K. Dalai and Y. Hu, *J. Clean. Prod.*, 136499 (2023).
51. A. Na Rungsi, A. Luengnaruemitchai, N. Chollacoop, S.-Y. Chen, T. Mochizuki, H. Takagi and Y. Yoshimura, *Fuel*, **331**, 125919 (2023).
52. N. N. A. Rasid, N. H. A. Khalid, A. Mohamed, A. R. Mohd.Sam, Z. A. Majid and G. F. Huseien, *J. Build. Eng.*, **65**, 105617 (2023).
53. M. N. Younis, Z. Ren, C. Li, E. Wang and J. Li, *Catalysts*, **13** (2023).
54. S. Musić, N. Filipović-Vinceković and L. Sekovanić, *Brazilian J. Chem. Eng.*, **28**, 89 (2011).
55. C. T. Ivan-Tan, A. Islam, R. Yunus and Y. H. Taufiq-Yap, *J. Clean. Prod.*, **148**, 441 (2017).
56. H. V. Lee, J. C. Juan, N. F. Binti Abdullah, R. Nizah Mf and Y. H. Taufiq-Yap, *Chem. Centr. J.*, **8**, 30 (2014).
57. Y. H. Taufiq-Yap, H. V. Lee, M. Z. Hussein and R. Yunus, *Biomass Bioenergy*, **35**, 827 (2011).
58. H. R. Mahmoud, *Fuel*, **256**, 115979 (2019).
59. F. Shahbazi, V. Mahdavi and J. Zolgharnein, *J. Iran. Chem. Soc.*, **17**, 333 (2020).
60. M. D. Putra, Y. Ristianingsih, R. Jelita, C. Irawan and I. F. Nata, *RSC Adv.*, **7**, 55547 (2017).
61. Z. Huang, F. Cui, H. Kang, J. Chen, X. Zhang and C. Xia, *Chem. Mater.*, **20**, 5090 (2008).
62. O. Rico-Fuentes, E. Sánchez-Aguilera, C. Velasquez, R. Ortega-Alvarado, J. C. Alonso and A. Ortiz, *Thin Solid Films*, **478**, 96 (2005).
63. M. Agarwal, G. Chauhan, S. P. Chaurasia and K. Singh, *J. Taiwan Inst. Chem. Eng.*, **43**, 89 (2012).
64. A. R. Gupta, S. V. Yadav and V. K. Rathod, *Fuel*, **158**, 800 (2015).